Nearly hyperuniform network models of amorphous silicon

Miroslav Hejna,[1,*] Paul J. Steinhardt,[1,2,†] and Salvatore Torquato[1,3,‡]
[1]*Department of Physics, Princeton University, Princeton, New Jersey 08544, USA*
[2]*Princeton Center for Theoretical Science, Princeton University, Princeton, New Jersey 08544, USA*
[3]*Department of Chemistry, Princeton Institute for the Science and Technology of Materials, and Program in Applied and Computational Mathematics, Princeton University, Princeton, New Jersey 08544, USA*
(Received 3 March 2013; published 17 June 2013)

We introduce the concept of *nearly hyperuniform network* (NHN) structures as alternatives to the conventional continuous random network (CRN) models for amorphous tetrahedrally coordinated solids, such as amorphous silicon (a-Si). A hyperuniform solid has a structure factor $S(k)$ that approaches zero as the wavenumber $k \to 0$. We define a NHN as an amorphous network whose structure factor $S(k \to 0)$ is smaller than the liquid value at the melting temperature. Using a novel implementation of the Stillinger-Weber potential for the interatomic interactions, we show that the energy landscape for a spectrum of NHNs includes a sequence of local minima with an increasing degree of hyperuniformity [smaller $S(k \to 0)$] that is significantly below the frozen-liquid value and that correlates with other measurable features in $S(k)$ at intermediate and large k and with the width of the electronic band gap.

DOI: 10.1103/PhysRevB.87.245204 PACS number(s): 61.43.Dq, 71.23.Cq

I. INTRODUCTION

The development of accurate structural models of amorphous silicon (a-Si) and other tetrahedrally coordinated solids has been an active area of research for the last eight decades,[1–3] but many challenges remain. The structure of a-Si is approximated well by continuous random network (CRN) models,[2,3] the first of which was introduced by Zachariasen in 1932.[1] Conventional CRNs for a-Si are fully four-coordinated, isotropic disordered networks that contain primarily five, six, and seven atom rings, while maintaining nearly perfect local tetrahedral order (narrow bond-angle and bond-length distributions). Predictions derived from CRN models assuming a Keating potential describes the interatomic interactions are in good agreement with many structural properties of a-Si that are accessible via experiments, including the radial distribution function (RDF) and the phonon and electron density of states,[3–5] nearest- and next-nearest-neighbor distances, bond statistics, ring statistics, etc. These successes are related to the form of the structure factor $S(k)$ at intermediate wavenumbers k.

In this article, we introduce the concept of *nearly-hyperuniform network* (NHN) structures and, on the basis of computer simulations, propose that NHN models may provide a better description of a-Si, especially after annealing. A perfectly *hyperuniform solid has a structure factor* $S(k)$ *that approaches zero as the wavenumber* $k \to 0$, implying that infinite-wavelength density fluctuations vanish.[6] The CRN models based on the Keating model that have been considered in the past (e.g., Ref. 4) have values of $S(k \to 0)$ comparable to those found in the liquid phase at the equilibrium melting temperature, $S(k \to 0) \approx 0.03$. We define a *nearly hyperuniform network as a disordered tetrahedral structure whose* $S(k \to 0)$ *is less than the liquid value at melting.* As a practical matter, we shall be interested in cases where $S(k \to 0)$ is substantially less, by 50% or more, which implies a substantial reduction in the large-scale density fluctuations and runs counter to the limitations imposed by the frozen-liquid paradigm.

Employing a novel simulation protocol that is based on the Stillinger-Weber (SW) potential to model the interatomic interactions, we generate a spectrum of NHN models and show that the energy landscape includes a sequence of progressively more hyperuniform minima with values $S(k \to 0)$ that are substantially less than the melting value—by a factor of 2 or more. We further show that the degree of hyperuniformity correlates with other measurable signatures in $S(k)$ at intermediate and large k and with the width of the electronic band gap. The simulations suggest that the sequence of states can be reached through extensive annealing, and more efficiently when combined with pressure. Companion experiments on a-Si will be reported elsewhere[7] that lend support to this picture.

While the SW potential has been shown to give a more realistic description of crystalline silicon,[8] the energy penalty for dangling bonds is not sufficiently large, and hence quenches from the melt, via molecular dynamics, result in an unrealistic number of coordination defects. These defects are avoided in conventional CRN models by using the less realistic Keating potential that enforces perfect fourfold coordination.

II. METHODS

In our study, we have devised a novel two-step numerical protocol to produce a spectrum of NHN models that combines the advantages of the Keating and SW potentials. Step one is a standard bond-switching annealing procedure using a Keating potential[9] applied to 20 000 atoms within a cubic box (under periodic boundary conditions) that is augmented with procedural modifications introduced by Barkema and Mousseau (BM).[4,10] However, unlike the BM CRN model, we anneal our systems significantly longer (between 2 to 250 times as long as measured by the number of accepted transpositions) to achieve a sequence of inherent structures (local potential-energy minima) that have lower energies than those of the BM model. In the second step of our procedure, we use our end-state inherent-structure configurations obtained via a Keating potential (K1, K2, etc.) as *initial conditions* for atomic-position rearrangement under a modified SW potential[5,11] at zero pressure via a conjugate gradient method. We label the corresponding inherent structures of this SW potential respectively SW1, SW2, etc. With this two-step

procedure, the resulting structures possess a negligible number of dangling bonds.

The first step of our two-step procedure involves producing a highly annealed CRN model based on the Keating potential as an initial condition for a SW quench. Barkema and Mousseau used an accelerated and scalable modification of the Wooten, Winer, and Weaire (WWW) technique[12] to produce large Keating-relaxed CRN models that have been a standard in the field. We have introduced several improvements to the Barkema-Mousseau algorithm, which, together with faster computers, allow us to generate significantly higher quality CRNs.

The starting point of the WWW technique is a disordered, perfectly four-coordinated network of atoms in a periodic box. Following the suggestion by Barkema and Mousseau,[4] we started from a liquid-like configuration to avoid any memory of an initial crystalline state. This disordered network is evolved through a sequence of bond switches that are accepted with Hastings-Metropolis acceptance probability

$$P = \min[1, \exp(-\Delta E_s / k_B T)],$$

where k_B is the Boltzmann constant, T is the temperature, and ΔE_s is the change of energy due to the bond switch, evaluated from the Keating potential:[13]

$$E_{\text{Keat.}} = \frac{3}{16}\frac{\alpha}{d^2}\sum_{i,j}(\mathbf{r}_{ij}\cdot\mathbf{r}_{ij} - d^2)^2 + \frac{3}{16}\frac{\beta}{d^2}\sum_{i,j,k}\left(\mathbf{r}_{ij}\cdot\mathbf{r}_{ik} + \frac{1}{3}d^2\right)^2.$$

Here α, β are the bond-stretching and bond-bending constants respectively, and d is the equilibrium bond length.

Since the acceptance rate is less than 0.1% in a well annealed network, it is important to avoid a complete relaxation of trial configurations and reject the proposed move as soon as it becomes clear that the move will be rejected. To that end, Barkema and Mousseau have proposed that a move be rejected if the Keating force exceeds a certain threshold value.[4] In addition, we introduce here a *multiscale local cluster relaxation* methodology, which consists of the following steps:

(1) Only atoms in a small cluster of about 120 atoms around a switched bond are relaxed, with the bond-switch being rejected if the energy increases by more than a threshold value of 0.01 eV per atom in the cluster.

(2) If not rejected in step (1), atoms in a larger cluster of about 320 atoms around the switched bond are relaxed, with the bond-switch being accepted or rejected based on the Hastings-Metropolis acceptance probability.

(3) Relaxation of all the atoms is performed after about a hundred accepted moves to relieve any built up stress due to the local relaxation.

Performing only local relaxations is crucial to the scalability of the algorithm, while using multiple scales increases efficiency. An important speed-up is achieved by parallelization. We use an asynchronous master-worker parallelization paradigm, where the master proposes transpositions and workers report on their success, instead of a bulk synchronous parallelization proposed by Vink *et al.*[10]

In our procedure, the annealing temperature is slowly decreased from about 0.3 eV to about 0.15 eV per silicon atom. Following Barkema and Mousseau, we performed a zero-temperature quench every several thousand successful transpositions at the annealing temperature. During the annealing-quenching procedure, we varied the ratio of the two-body and three-body interaction by 5% and the volume of the system by 3%. We found that a significant speed-up of the quenches can be achieved by preferentially trying switching bonds that have the highest strain and the bonds that lie in the neighborhood of previously successful bond-switches, since the successful bond-switches often appear in clusters. Several models K1–K5 at various degree of annealing were produced whenever the Keating energy per atom showed a substantial decrease.

The second step of our two-step procedure to create a NHN model involves finding a zero-pressure inherent structure (local minimum) associated with a modified SW potential interaction using the aforementioned Keating configuration as an initial condition. The SW potential[8] involves two- and three-body interactions of the following form:

$$E_{SW} = \sum_{i,j} v_2(r_{ij}) + \sum_{i,j,k} v_3(r_{ij}, r_{ik}, \cos\theta_{ijk}),$$
$$v_2(r_{ij}) = \varepsilon f_2(r_{ij}/\sigma),$$
$$v_3(r_{ij}, r_{ik}, \cos\theta_{ijk}) = \varepsilon f_3(r_{ij}/\sigma, r_{ik}/\sigma, \cos\theta_{ijk}),$$

where

$$f_2(r) = \begin{cases} A(Br^{-p} - r^{-q})\exp[(r-a)^{-1}], & r < a, \\ 0, & r \geqslant a, \end{cases}$$
$$f_3(r_{ij}, r_{ik}, \cos\theta_{ijk}) = \lambda \exp[\gamma(r_{ij}-a)^{-1} + \gamma(r_{ik}-a)^{-1}]\left(\cos\theta_{ijk} + \frac{1}{3}\right)^2,$$

where $\varepsilon = 1.6483$ eV, $A = 7.050$, $B = 0.6022$, $p = 4$, $q = 0$, $a = 1.80$, $\lambda = 31.5$, $\gamma = 1.20$, and $\sigma = 2.0951$ Å are parameters that were determined from fitting the location of transverse optic and transverse acoustic peaks to neutron scattering experiments on a-Si by Vink *et al.*[5]

The structure factors $S(k)$ of the generated samples were evaluated by the *sampling volume* method. This method is based on the scaling behavior of density fluctuations presented by Torquato and Stillinger[6] and described in detail by de Graff and Thorpe.[14] It can be viewed as a Fourier transform of the pair-correlation function $g(r)$ with an appropriately chosen convergence factor that reduces artifacts due to the finite size of the model.[14]

III. RESULTS

In Fig. 1, we show $S(0)$ as a function of the inverse of the height H of the first scattering peak in $S(k)$ for K (BM), the Barkema-Mousseau CRN model[14] as well as for K3, K5, SW3, and SW5.[15] Importantly, it can be observed that the K (BM) model is not an endpoint of annealing under the Keating potential, since further annealing produces a sequence K1 through K5 along a trajectory where $S(0)$ gets smaller and the first peak height in $S(k)$ gets larger. Moreover, the models obtained by then quenching under the SW potential are nearly

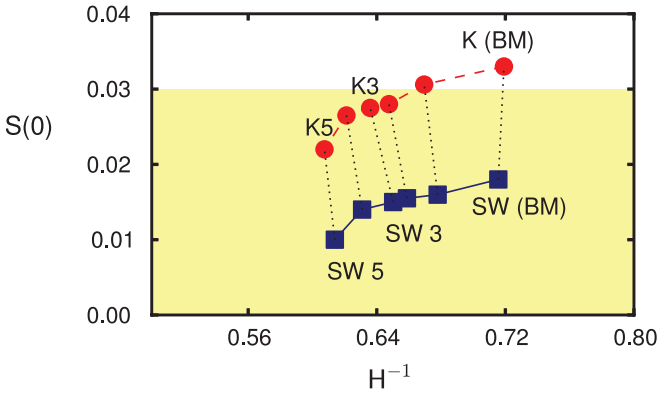

FIG. 1. (Color online) $S(0)$ vs the inverse height H of the first scattering peak for the K (BM) Keating annealed continuous random network model (Ref. 14) and our Keating annealed models (circles) and the corresponding Stillinger-Weber quenched models (squares). The shaded region indicates the nearly hyperuniform range in which $S(k \to 0)$ is below the equilibrium melting value for a-Si; note that the SW models are substantially below this threshold.

hyperuniform: they have values of $S(0)$ that extend to more than 50% lower than their K progenitors and substantially below the value at the melting temperature. They also have substantially higher radial distribution function (RDF) first-peak heights (see discussion of Tables I and II below). The most nearly hyperuniform structure obtained in our anneal run, SW5, yields $S(0) = 0.010 \pm 0.002$, which represents a 70% reduction in the large-scale density fluctuations relative to the BM model [$S(0) = 0.035 \pm 0.001$][14] or over three times more hyperuniform, which is a remarkably large reduction in the large-scale density fluctuations of the system. We note that we stopped with K5 because the annealing runs began to use unreasonable computational time; we believe that more refined hyperuniform amorphous networks are achievable with yet longer annealing times.

The SW5 model exhibits other signature features that correlate with increased hyperuniformity and can be measured experimentally:

(1) The SW5 structure possesses a bond-angle standard deviation that is more than a degree lower than that of the BM model and is in better agreement with recent bond-angle analysis of monatomic amorphous semiconductors.[16]

(2) The height of the first peak of $S(k)$ for the SW5 model is higher than for the BM model, as shown in Fig. 2(a).[17]

(3) The BM model has a significantly broader first peak in the RDF $g(r)$ (due to a larger bond-length variation) than the SW5, as shown in Fig. 2(b).

TABLE I. Short-ranged and long-ranged properties of the Keating-relaxed CRN models.

Model	σ_L	σ_A	$S(0)$	$g(r)$ Max
K (BM)	4.03%	9.94°	0.035	4.9
K1	3.84%	9.23°	0.031	5.1
K2	3.83%	9.14°	0.028	5.1
K3	3.80%	9.01°	0.027	5.2
K4	3.71%	8.71°	0.026	5.3
K5	3.64%	8.61°	0.022	5.4

TABLE II. Short-ranged and long-ranged properties of the NHN models.

Model	σ_L	σ_A	$S(0)$	$g(r)$ Max
SW (BM)	2.70%	10.5°	0.018	7.3
SW1	2.68%	10.0°	0.016	7.3
SW2	2.68%	9.8°	0.015	7.3
SW3	2.66%	9.6°	0.015	7.4
SW4	2.66%	9.3°	0.014	7.4
SW5	2.65%	9.2°	0.010	7.4

(4) For larger wavenumbers, the BM model predicts a significantly faster decay of the large-k oscillations in $S(k)$ than does that of the SW5 model,[15] as shown in Fig. 3.

(5) Based on a simulations of smaller 1000-atom models and using a tight-binding model for silicon by Kwon,[18] the electronic band gap increases with increasing hyperuniformity, as shown in Fig. 4. The width of the isotropic band gaps are calculated as the difference between the lowest energy state of the conduction band and the highest energy state of the valence band. The figure shows that the fractional band gap width $\Delta E/E$, increases as the SW energy per atom decreases, which correlates with increasing relaxation and thus the hyperuniformity. ΔE is the band gap width and E is the energy of the midpoint of the band gap compared to the lowest energy valence state. The same absolute gap width, ΔE, also increases with hyperuniformity.

Table I summarizes the structural properties of the Keating-relaxed CRN models with progressively higher level of annealing. K5, the most annealed model, has more than a degree lower bond angle deviation than Barkema-Mousseau models[4] [K (BM)]. The short-range order of the models

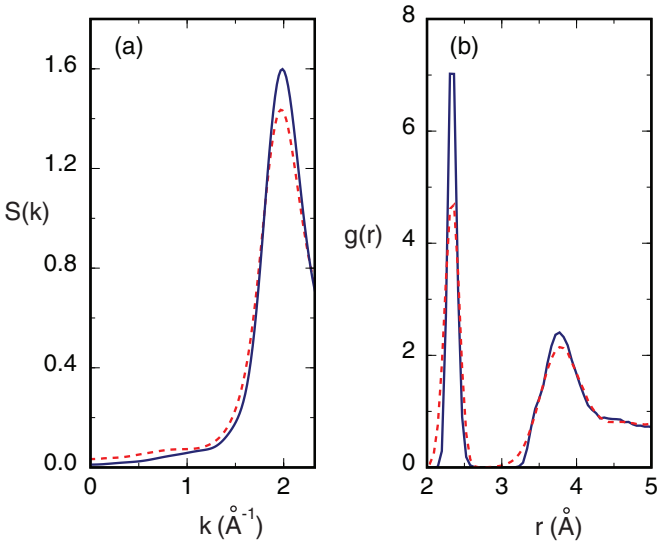

FIG. 2. (Color online) (a) Comparison of the angularly averaged structure factor $S(k)$ vs wavenumber k for small to intermediate k for the Stillinger-Weber quenched SW5 model (blue solid curve) and the Keating annealed K (BM) model (Ref. 4; red dashed line). (b) Comparison of the first peak in radial distribution function $g(r)$ vs radial distance r for the K (BM) model (Ref. 4; red dashed curve) and the SW5 model (blue solid curve).

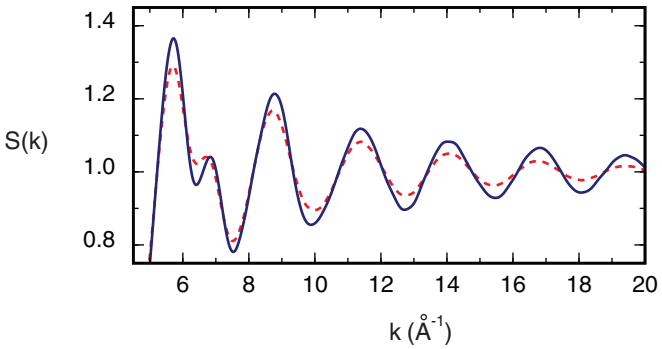

FIG. 3. (Color online) The angularly averaged structure factor $S(k)$ vs wavenumber k at large k for the Stillinger-Weber quenched SW5 model (blue solid curve) displays larger amplitude oscillations than the Keating-annealed K (BM) model (Ref. 4; red dashed curve).

improves with annealing. Table I shows the standard deviation σ_L of the bond length, standard deviation σ_A of the bond angle, limit of the structure factor as $k \to 0$, and the height of the first-coordination shell peak in $g(r)$.

Table II summarizes the structural properties of the NHN models derived from the CRN models by a zero-pressure minimization of the modified Stillinger-Weber potential. The SW (BM) model is obtained from the Barkema-Mousseau CRN model[4] [K (BM)]. Table II shows the standard deviation of the bond length, standard deviation of the bond angle, limit of the structure factor as $k \to 0$, and the height of the first-coordination shell peak in $g(r)$.

Table III compares the irreducible ring statistics of the Barkema-Mousseau CRN model[4] [K (BM)] and our most annealed model (K5). Medium-range order significantly improves with annealing, as seen by the increased number hexagons and smaller number of squares as well as 8 and 9 membered rings.

Table IV shows the average motion of atoms (measured by the configurational proximity metric $p_{12} = \sqrt{\sum_{k=1}^{N} |\mathbf{r}_{i,k} - \mathbf{r}_{f,k}|^2}/r_0$, where $r_{i,k}$, $r_{f,k}$ are the initial and final positions of atoms in the

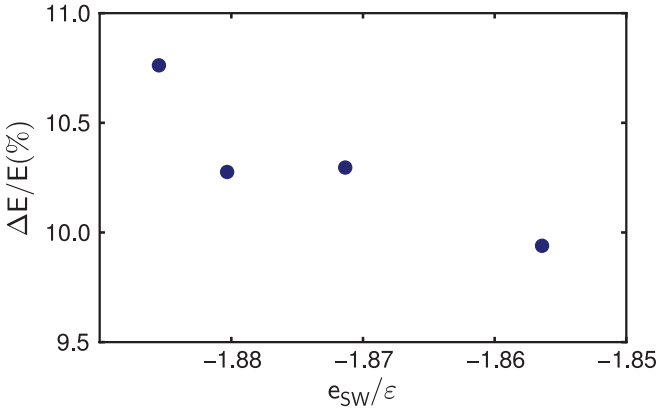

FIG. 4. (Color online) Fractional band gap, $\Delta E/E$ vs the average SW energy per atom e_{SW} in units of $\varepsilon = 1.6483$ eV, where ΔE is the band gap width and E the energy at the midpoint of the band gap (measured with respect to the bottom of the valence band). The value of e_{SW}/ε decreases with increasing hyperuniformity, as shown in Table IV below; hence, the figure shows that fractional band gap width increases with hyperuniformity.

TABLE III. Comparison of the ring statistics between the Barkema-Mousseau CRN model [Ref. 4; K (BM)] and our most annealed model (K5).

Ring order	4	5	6	7	8	9
K (BM)	2.39%	45.5%	74.1%	51.0%	15.7%	4.1%
K5	0.99%	42.8%	85.0%	53.9%	12.9%	2.6%

SW quench and r_0 is the mean nearest-neighbor distance[19]) as a result of replacing the Keating interaction with the Stillinger-Weber interaction. This quantifies the configurational distance of the SW models from their K progenitors. The Keating energy (e_K) and Stillinger-Weber energy per atom (e_{SW}) are shown for the K and corresponding SW model. The SW (BM) model is obtained from the Barkema-Mousseau CRN model[4] [K (BM)].

To ensure that our NHN configurations are truly amorphous, we analyzed them for the presence of ten-atom cages composed of four adjacent six-rings that constitute a basic building block of the diamond crystalline structure. Our results show that the most annealed CRN sample, K5, has 0.02 ten-atom cages per atom; a tiny fraction compared to the perfect crystal that has one ten-atom cage per atom. Since the Stillinger-Weber relaxation produces only negligible amount of topological defects, the results for K models carry over to the corresponding SW models. The ten-atom cages are quite uniformly distributed throughout the volume, and there are no large clusters. Comparison of our results to a recent study of nucleation[20] shows that NHN models are far from crystallization.

Table V shows characteristics of the ten-atom cages of our models. The results for a crystalline and paracrystalline[21] models are shown for reference. The first column shows the number of diamond cages per atom; the second column shows the number of clusters of diamond cages per atom; the third column shows the size of the maximal cluster; the fourth column shows the average of the clusters; and the fifth column shows the number of interior cages. *Interior cages* are defined as cages whose atoms and neighbors all lie within the same cluster. Clusters are collections of ten-atom cages in which each ten-atom cage shares one atom or more with at least one other ten-atom cage. Cage statistics of the K1-5 and SW1-5 models shows that while our models are significantly more

TABLE IV. Energies per atom of the K and SW models under different interactions. e_{SW} is given in units of the SW potential energy scale $\varepsilon = 1.6483$ eV. e_K is given in dimensionless units in which $d = \sqrt{3}/2$ and $\alpha = d^2$. Energies of the diamond lattice are shown for comparison. The first column shows the distance of a SW model from its K progenitor in terms of the proximity metric.

Model	Prox. metric	e_K (K)	e_{SW}/ε (K)	e_{SW}/ε (SW)
SW (BM)	0.723%	0.02130	−1.7809	−1.8264
SW1	0.900%	0.01864	−1.8141	−1.8505
SW2	1.062%	0.01833	−1.8179	−1.8532
SW3	0.952%	0.01794	−1.8235	−1.8553
SW4	1.088%	0.01685	−1.8372	−1.8645
SW5	1.015%	0.01648	−1.8421	−1.8660
Diamond		0	−2.0000	−2.0000

TABLE V. The table shows the number of ten-atom cages per atom (No. cages); the number of clusters (cl.) per atom; the number of atoms in the largest cluster; the average cluster size; and the number of interior cages. The K1-5 and SW1-5 models all contain 20,000 atoms; the crystalline has N and the paracrystalline model has 1728 atoms.

Model	No. cages	No. cl. per atom	Max cl.	Aver. cl.	No. int. cages
K/SW (BM)	0.9%	6.29×10^{-3}	40	12.6	0
K1/SW1	1.6%	8.30×10^{-3}	77	14.4	0
K2/SW2	1.6%	8.20×10^{-3}	87	14.6	2
K3/SW3	1.6%	8.10×10^{-3}	88	14.9	0
K4/SW4	1.9%	9.15×10^{-3}	48	15.5	0
K5/SW5	2.2%	9.95×10^{-3}	90	15.7	0
Paracryst.	15.5%	4.05×10^{-3}	746	122.7	67
Diamond cryst.	100%	$1/N$	N	N	N

relaxed than the BM model, the models are very far from crystallinity or paracrystallinity.

Table VI shows values of $S(0)$ for a sequence of models that were obtained by a constant volume SW quench of CRN5 at various degrees of compression. Compression is expressed in terms of the relative compression of the linear scale compared to the linear scale of the sample at zero pressure (SW5). The uncertainty of $S(0)$ is 0.002.

IV. DISCUSSION

The fact that our annealing-quenching procedure produces a sequence of NHN models with an increasing degree of hyperuniformity [i.e., $S(0)$ tending to zero] has deep significance. First, it demonstrates that the energy landscape for conventional Keating-annealed CRN models, for Stillinger-Weber quenched models, and, hence, probably amorphous silicon, has local minima that span a greater diversity of structures than was previously recognized. It also demonstrates that, experimentally, it is possible to reach minima that are more nearly hyperuniform than had been thought achievable. The density fluctuations as measured by $S(0)$ are not frozen at the freezing point, but continue to decrease with annealing. In particular, the value of $S(0)$ cannot be considered a universal quantity for a-Si or any other amorphous tetrahedral network, as might be inferred from de Graff and Thorpe.[14] For example, while the percentage drop in the energy per atom in going from the K (BM) model to SW5 is about 23%, the corresponding drop in $S(0)$ is about 50%. Remarkably, the *configurational proximity metric*,[19] which gauges the average local atomic movement required to transform one structure into another, is only about one percent of a bond-length with a corresponding percentage energy drop of only about 2.4% during our Stillinger-Weber (framework) quenching step from a Keating potential-annealed CRN to a SW potential-quenched NHN state, even though the latter possesses an $S(0)$ that is about one-half the CRN value. This reveals the importance of collective atomic rearrangements during the second step of our quenching protocol.

TABLE VI. Dependence of $S(0)$ on the relative compression of the linear scale during a constant-volume SW quench.

Rel. Compr.	−4%	0%	4%	8%
P (GPa)	−10	0	10	30
$S(0)$	0.017	0.010	0.009	0.007

Our findings are completely consistent with recent results for amorphous metals in which the atomic pair interactions are isotropic.[22,23] In these studies, it has been demonstrated that, on approach to an inherent structure, $S(0)$ is nearly hyperuniform and decreases monotonically,[22] and that $S(0)$ decreases as the temperature decreases, i.e., as deeper local minima in the energy landscape are accessed.[23] Thus, the observation that sampling deeper energy minima are accompanied by increased hyperuniformity appears to apply to a wide class of disordered systems (with both isotropic and directional interactions) and its full elucidation demands attention in the future.

Is it possible to construct a-Si with appreciably smaller $S(0)$ than reported here or, more ambitiously, reach true hyperuniformity [$S(k \to 0) = 0$]? There are both fundamental and practical reasons to consider such questions. On the practical side, our results above suggest that hyperuniform amorphous tetrahedral network models will have larger electronic band gaps than typical non-hyperuniform samples.[2] Similar ideas have successfully led to the creation of novel designer materials composed of a hyperuniform disordered arrangement of dielectric materials that have complete photonic band gaps.[24–27] On the theoretical side, our present computational results strongly indicate that continued annealing of a-Si samples improves the degree of hyperuniformity. Moreover, our simulations suggest that quenching a-Si samples under increased pressure leads to further decrease of $S(0)$ [see Table VI for dependence of $S(0)$ on compression].

Perfect hyperuniformity has been observed previously in disordered systems with hard, short-range isotropic interactions, most notably in a wide class of maximally random jammed packings.[28,29] It has also been found in systems with soft, long-range interactions; for example, in one component plasmas[30,31] or in the ground states of so-called *stealthy* potentials[32] that enforce $S(k) = 0$ for a k in a range $[0, k_C]$, where $k_C > 0$. The existence of these diverse examples and our construction here of a sequence of increasingly hyperuniform configurations suggests that the search for a configuration with $S(k \to 0) = 0$ is one of the exciting areas for future research.

Even before our numerical studies of NHN models began, the general theoretical conjectures above stimulated recent measurements by Xie *et al.*[7] of the structure factor in the long-wavelength limit for a sample of a-Si synthesized by direct ion bombardment. These experiments have measured $S(k \to 0)$ to determine the degree of hyperuniformity both as-implanted and after annealing and have also checked several other correlated signatures predicted above. The results are reported elsewhere.[7]

ACKNOWLEDGMENTS

We are grateful to Gabrielle Long and Sjoerd Roorda for testing the theory and suggesting possible experimental signatures. We also Marian Florescu, Frank Stillinger, and Étienne Marcotte for very helpful discussions. S.T. was supported by the Office of Basic Energy Sciences, Division of Materials Sciences and Engineering under Award No. DE-FG02-04-ER46108.

*mhejna@princeton.edu
†steinh@princeton.edu
‡torquato@princeton.edu

[1]W. H. Zachariasen, J. Am. Chem. Soc. **54**, 3841 (1932).
[2]R. Zallen, *The Physics of Amorphous Solids* (Wiley, New York, 1998).
[3]N. Mousseau, G. T. Barkema, and S. M. Nakhmanson, Philos. Mag. B **82**, 171 (2002).
[4]G. T. Barkema and N. Mousseau, Phys. Rev. B **62**, 4985 (2000).
[5]R. Vink, G. Barkema, W. van der Weg, and N. Mousseau, J. Non-Cryst. Solids **282**, 248 (2001).
[6]S. Torquato and F. H. Stillinger, Phys. Rev. E **68**, 041113 (2003).
[7]R. Xie *et al.* (unpublished).
[8]F. H. Stillinger and T. A. Weber, Phys. Rev. B **31**, 5262 (1985).
[9]B. R. Djordjević, M. F. Thorpe, and F. Wooten, Phys. Rev. B **52**, 5685 (1995).
[10]R. L. C. Vink, G. T. Barkema, M. A. Stijnman, and R. H. Bisseling, Phys. Rev. B **64**, 245214 (2001).
[11]We use the same parameters of the SW potential that were determined by fitting the phonon spectra of a-Si to neutron scattering data (Ref. 5).
[12]P. N. Keating, Phys. Rev. **145**, 637 (1966).
[13]F. Wooten, K. Winer, and D. Weaire, Phys. Rev. Lett. **54**, 1392 (1985).
[14]A. M. R. de Graff and M. F. Thorpe, Acta Crystallogr. A **66**, 22 (2010).
[15]We thank S. Roorda and G. Long for suggesting these tests.
[16]S. Roorda, C. Martin, M. Droui, M. Chicoine, A. Kazimirov, and S. Kycia, Phys. Rev. Lett. **108**, 255501 (2012).
[17]The NHN5 model exhibits a small scattering enhancement near $k = 1$ Å^{-1} seen in the experiments of Ref. 7.
[18]I. Kwon, R. Biswas, C. Z. Wang, K. M. Ho, and C. M. Soukoulis, Phys. Rev. B **49**, 7242 (1994).
[19]R. D. Batten, F. H. Stillinger, and S. Torquato, J. Chem. Phys. **135**, 054104 (2011).
[20]P. Beaucage and N. Mousseau, Phys. Rev. B **71**, 094102 (2005).
[21]MC R TDV model; M. M. J. Treacy and K. B. Borisenko, Science **335**, 950 (2012).
[22]A. B. Hopkins, F. H. Stillinger, and S. Torquato, Phys. Rev. E **86**, 021505 (2012).
[23]É. Marcotte, F. H. Stillinger, and S. Torquato, J. Chem. Phys. **138**, 12A508 (2013).
[24]M. Florescu, S. Torquato, and P. J. Steinhardt, Proc. Natl. Acad. Sci. **106**, 20658 (2009).
[25]M. Florescu, S. Torquato, and P. J. Steinhardt, Phys. Rev. B **80**, 155112 (2009).
[26]M. Florescu, S. Torquato, and P. J. Steinhardt, Appl. Phys. Lett. **97**, 201103 (2010).
[27]W. Man *et al.* (unpublished).
[28]A. Donev, F. H. Stillinger, and S. Torquato, Phys. Rev. Lett. **95**, 090604 (2005).
[29]C. E. Zachary, Y. Jiao, and S. Torquato, Phys. Rev. E **83**, 051308 (2011); **83**, 051309 (2011).
[30]J. L. Lebowitz, Phys. Rev. A **27**, 1491 (1983).
[31]S. Torquato, A. Scardicchio, and C. E. Zachary, J. Stat. Mech. (2008) P11019.
[32]R. D. Batten, F. H. Stillinger, and S. Torquato, J. Appl. Phys. **104**, 033504 (2008).